

Trajectory of Particles Rebounding Off Plane Targets

J. D. Armstrong,* N. Collings,† and P. J. Shayler‡
University of Nottingham, United Kingdom

An experimental rig and procedure is described, which is used to determine the distribution of air-borne particles rebounding from a target. The particles used are angular coal particles, screened to 125-150 μm , impinging on commercial stainless steel and aluminum alloy targets at ~ 140 m/s, and at various incident angles; after impact, the mean particle trajectory is found to be curved. An approximate form of trajectory equation is derived, and fitted to the data points in order to determine the true value of rebound angle for each trajectory. The change in direction of the mean particle path is found to be up to 30 deg, depending on the incident angle. The evidence that trajectories are curved indicates that care must be exercised when using double-flash photographic methods to obtain information.

Introduction

THE behavior of particles impinging on and rebounding off surfaces has great practical relevance to erosion and deposition problems associated with particle laden gas flows. In the last twenty years in particular, much effort has been invested in the study of particulate laden gas flows through gas turbines prompted by the use of aircraft in desert areas, for example. More recently, there has been growing interest in the use of gas turbines driven by the flue gas from fluidized bed coal combustors. In these applications, erosion and deposition can lead to unacceptable performance degradation.

The prediction of how particulate burdens will affect turbine performance is an exacting task. A number of computer codes have been developed to predict how particles will behave as they pass through the turbine. Generally, however, they depend on empirical data for impingement behavior to predict rates and patterns of erosion. Furthermore, the data provide insight to the mechanisms of erosion, which are still poorly understood.

In a series of papers, Tabakoff et al.¹⁻³ describe the results of theoretical and experimental studies of the erosion of metal surfaces by impinging particles. In an effort to characterize the erosion mechanism, the variation of erosion rate with the speed and direction of the particles as they impinge and as they leave the target have been measured. The investigations were conducted using a confined-flow rig in which particles were seeded into the flow well upstream of the working section containing targets inclined at an angle to the nominal flow direction.

One disadvantage of this is that spatial variations in flow conditions are large in the vicinity of the target. The information obtained reflects flowfield effects as well as impingement phenomena and these are difficult to distinguish. A second disadvantage is the restricted access in the vicinity of the surface and the need to use nonintrusive experimental techniques to avoid flow disturbances. Tabakoff et al. have used cine-photography to good effect to this end, but the technique is time consuming and requires careful control of experimental conditions, particularly the particulate concentration, to obtain good results.

In the work reported here, a different approach has been adopted. The trajectory of angular coal particles rebounding from plane metal surfaces have been studied experimentally using a simple and effective capture technique. The size of particles was in the range 125-150 μm . Much of the current research into gas-borne particle interactions is addressed to the fluidized bed combustor situation, where particles an order of magnitude smaller than those used in the present paper need to be considered. The effects of particle spin are much easier to examine experimentally using larger particles, though it is expected that the trends observed will be relevant to smaller particles. In a real gas turbine, for example, the results of this work would enable an estimate to be made of the relative importance of spin induced effects.

Two target materials have been used, namely, stainless steel and aluminum. The experiments were conducted in essentially quiescent air to minimize the effects of air motion on the particle trajectories. The incident particle velocity was maintained constant at approximately 140 m/s and the effect of angle of incidence on rebound angle has been examined.

The results show that the trajectory of rebounding particles is curved. The reason for this is explored theoretically on the basis that the particles are spinning after impact and experience a lift force acting normal to the direction of flight. A simple model is described and is shown to give results consistent with the experimental data.

Experimental Investigation

The hopper feed system shown in Fig. 1, which is similar to a system described by Tabakoff,² was used to generate a

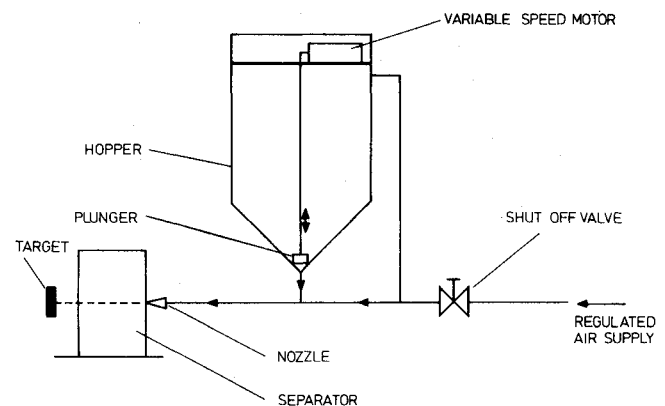


Fig. 1 Schematic of continuous flow system.

Received Oct. 8, 1982; revision received April 11, 1983. Copyright © American Institute of Aeronautics and Astronautics, Inc., 1983. All rights reserved.

*Research Assistant, Department of Mechanical Engineering.

†Lecturer, University Engineering Department, Cambridge, U.K.

‡Lecturer, Department of Mechanical Engineering.

particle laden air stream. The stream is accelerated through a long, fine bore nozzle of 2-mm diameter and fed to a flow separator, Fig. 2, which produces a jet of particles with a small angle of divergence. Most of the slower moving particles, and the bulk of the air flow, is removed by the two spatial filters. Downstream of the filters, the particle concentration was low and particle-particle interaction was negligible.

The feed system pressure was fixed at 2.5×10^5 Pa for all the tests, to produce choked flow at the nozzle exit. The particle stream's average velocity was measured using a simple pendulum placed at the target position. The difference in the position of the pendulum with and without particle feed, but with the (slight) air stream in both cases, was measured. Using a previously obtained figure for the mass flow rate, the average particle velocity was obtained as 130 m/s.

A new target, with a polished surface, was used for each test. The particles used were of pulverized coal, screened to between 125 and 150 μm .

The sampling of rebounding particles at various positions relative to the target was achieved using double-sided tape as the collector to which incident particles attach themselves. After a test the tape was examined under a microscope, and the number of particles in each 5-mm strip was counted. The results of such an experiment are shown in Fig. 3. The most likely trajectory was taken as the weighted mean. Tests were conducted using aluminum and stainless steel targets, with $10^\circ < \beta_1 < 50^\circ$ and $40 \text{ mm} < x < 350 \text{ mm}$. The trajectory parameters are defined in Fig. 7.

To assess the results, histograms were plotted for various values of x as exemplified in Fig. 3. From these, the mean particle trajectory could be plotted. An example is shown in Fig. 4, which is typical, and clearly shows the curved nature of the trajectory. It is to be emphasized that air motion was not responsible for this behavior. Smoke investigations in this region did not show any significant air motion in the region of the target. The best fit line in Fig. 4 is a least squares fit to an equation of the form devised in the following section.

In Figs. 5 and 6 the values of β_2/β_1 have been plotted against β_1 for stainless steel and aluminum. Also in Figs. 5 and 6 the results of Tabakoff³ have been plotted for stainless steel and aluminum.

Theory

From the results presented later in this paper, it appears probable that a significant lift force is present on particles

rebounding from the target. In this section, the particle trajectory is investigated assuming that the Magnus force is responsible for the lift.

For the particles under study here, which have a radius a of $\sim 75 \mu\text{m}$, and velocities U in the range 50-100 m/s, the Reynolds number range will be 250-500, based on diameter. Data for drag, drag torque, and lift is not readily available for this range of Re , and especially not for rough spheres. The drag coefficient may be expected to be in the range 0.6-1.0, based on the relationships for smooth spheres.

We wish to know, initially, if we can neglect the change in U due to linear drag. To do this let us assume that C_D is constant, and neglect spin effects.

It is convenient here to define axis X, Y , where X is the initial direction of the rebounding particle (see Fig. 3).

Now,

$$\frac{md^2X}{dt^2} = -C_D \frac{1}{2} \rho U^2 \pi a^2$$

so

$$\frac{U}{U_0} = \exp\left(-C_D \frac{\pi \rho a^2 X}{2m}\right) \quad (1)$$

where U_0 is the initial velocity, and m the particle mass. The density of the particles was about 1500 kg/m^3 , and their mean radius $\approx 75 \mu\text{m}$. C_D for smooth, nonrotating spheres at the relevant Reynolds numbers is about 0.8. We, therefore, obtain

$$U/U_0 = \exp(-X/0.35)$$

Over the trajectory lengths of interest, i.e., up to about 0.4 m, the velocity of the particles will have reduced considerably. Nevertheless, since we are not concerned here with the time history of the trajectory, the velocity of the particles can be assumed to be constant. This assumption can be justified by noting that the lift force is approximately proportional to the particle velocity. Over the distances involved, the effect on the predicted trajectory will be small compared with the experimental errors. The advantage in making this assumption is that a convenient mathematical description of the particle trajectory is possible.

The lift force to the Magnus effect on a sphere can be expressed as

$$F = k_1 a^3 \rho \omega U \quad (2)$$

where ω is the angular velocity and k_1 a dimensionless quantity. Interpretation of the results of Maccoll,⁴ which were

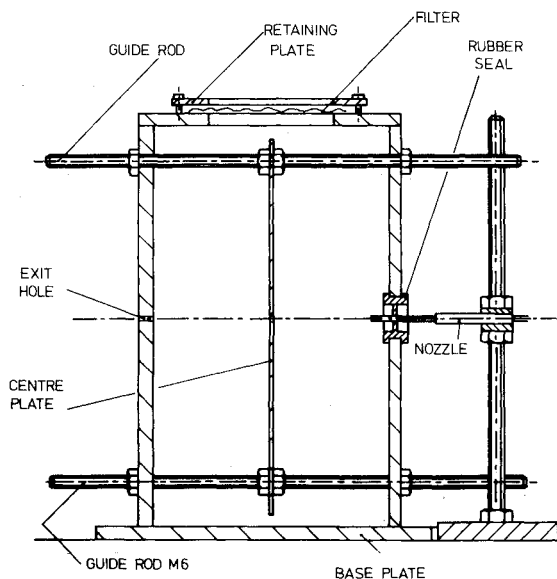


Fig. 2 Air/particle flow separator.

TEST DETAILS

TARGET MATERIAL ---- ALUMINUM
ANGLE OF INCIDENCE -- 11 DEG
COLLECTOR DISTANCE -- 125 MM

TOTAL MOMENT ---- 11760
TOTAL COUNT ---- 2232
MEAN Y VALUE ---- 5.27

EXPERIMENTAL DATA

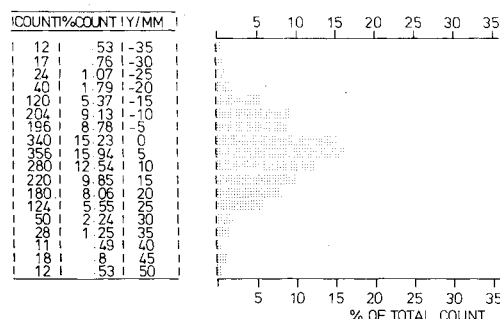
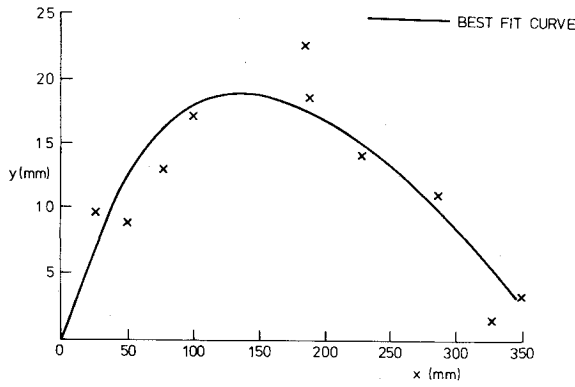
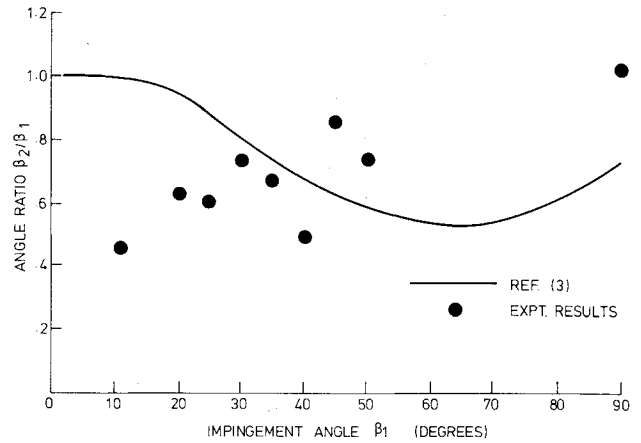
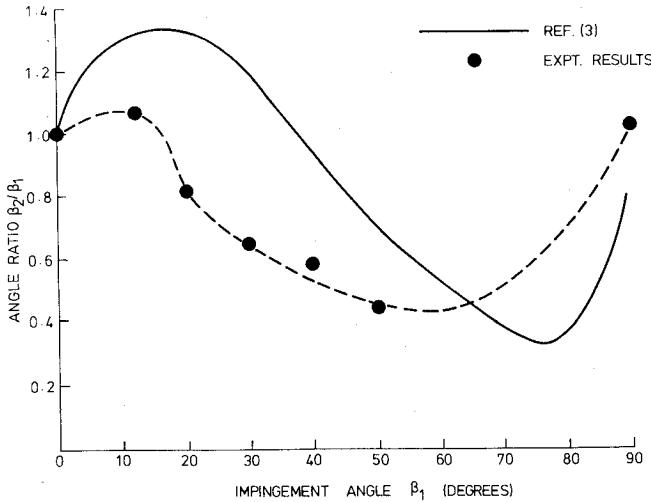


Fig. 3 Typical particle distribution at collection system.

Fig. 4 Trajectory for $\beta_I = 30$ deg, aluminum target.Fig. 6 Impingement angle ratio (β_2/β_1), aluminum targets.Fig. 5 Impingement angle ratio (β_2/β_1), stainless steel targets.

for $Re \approx 10^5$, gave $k_1 = \pi/10$ when $\omega \cdot a > U/2$, and Rubinow and Keller⁵ found $k_1 = \pi$ for $Re \leq 1$. We will assume here that it is a constant to be found by matching predictions to theory.

The drag torque may be expressed as

$$T = -k_2 \cdot \rho a^3 \nu \cdot \omega \quad (3)$$

k_2 , like k_1 , is dimensionless, and it is shown by Rubinow and Keller that $k_2 = 8\pi$, for $Re \leq 1$. For spheres spinning in a stationary fluid, experiments by Sawatzki⁶ show that for $Re \leq 100$, $T \propto \omega^{4/3}$. Since the power of ω is not very different from unity, a constant k_2 will be assumed here and the value deduced from experiment.

Since it is found experimentally that the change in trajectory direction in the region of study is less than 30 deg, the analysis can be simplified by assuming that the lift force always acts in the $-ve Y$ direction.

Equation (3) can be solved to give

$$\omega = \omega_0 \exp\left(\frac{-k_2 \rho a^3 \nu}{I} T\right)$$

where ω_0 is the initial angular velocity and I the particle's moment of inertia.

The Cartesian equation of motion can now be expressed as

$$m \frac{d^2 X}{dt^2} = 0 \quad \text{i.e.,} \quad \frac{dX}{dt} = U_0$$

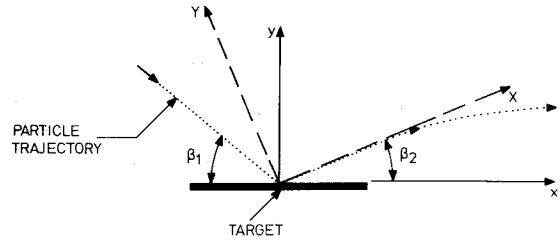


Fig. 7 Coordinate system and impact parameters.

and

$$m \frac{d^2 Y}{dt^2} = -k_1 a^3 \rho \omega_0 U_0 \exp\left(\frac{-k_2 \rho a^3 \nu}{I} t\right)$$

Integrating twice, with the boundary conditions

$$\frac{dY}{dt} = Y = 0 \quad \text{for} \quad t = 0$$

we find

$$Y = AB[1 - e^{-X/B}] - XA \quad (4)$$

where

$$A = \frac{Ik_1 \omega_0}{mk_2 \nu} \quad (5a)$$

$$B = \frac{IU_0}{k_2 \rho a^3 \nu} \quad (5b)$$

and the substitution $U_0 = Xt$ has been made. Referring to the x, y axes, defined in Fig. 7, putting $\tan \theta = A$, and noting that for these experiments $x \cos \beta_2 \gg y \sin \beta_2$, we finally obtain

$$y = -x \tan(\theta - \beta_2) + \frac{B \tan \theta [1 - \exp(-\cos \beta_2 x/B)]}{\cos \beta_2 (1 + \tan \theta \tan \beta_2)} \quad (6)$$

Clearly, $(\theta - \beta_1)$ expresses the final trajectory direction for large x , and B is a "distance constant" expressing the distance over which the Magnus force is important. It is shown subsequently that the form of Eq. (6) is consistent with available experimental and theoretical data.

Discussion

Equation (6) has been used to make a least squares fit to the experimental data. Tables 1 and 2 show that total deflections θ

of up to 50 deg might be expected from the initial direction after impingement, although measurements have only been made up to the point on the trajectory deviation up to about 30 deg.

Stainless Steel

The tabulated results illustrate a virtually constant final turning angle θ of about 40 deg for stainless steel, suggesting that the initial spin ω_0 is largely independent of incident angle β_1 , if the values of k_1 and k_2 are assumed to be constant. Similarly the value of B , the distance constant, is approximately constant for stainless steel, suggesting that the rebound velocity U_0 is also independent of β_1 . This conclusion is in agreement with the results of Tabakoff,³ whose measurements show that for 15 deg $< \beta_1 < 50$ deg, U_0 varies by less than 10%. Finally, the variation of β_2/β_1 with β_1 shows similar trends to those measured by Tabakoff, in particular, the increase in β_2/β_1 above unity at small values of β_1 .

Aluminum

The results for aluminum are not as good as those for stainless steel in the sense that there was much more scatter in both experimental points describing the particle trajectory; and, consequently, curve fitting was less satisfactory. Nevertheless, the results are again broadly in agreement with those of Tabakoff for the variation of β_2/β_1 with β_1 .

The variation of θ , the total turning angle, is greater than that for stainless steel. There is a definite trend of increasing θ with β_1 at small angles of incidence, suggesting that, in this range, ω_0 increases with β_1 . It might be argued that the particle is "skidding" at small angles of incidence and not spinning up during impact. The large variations in B , particularly at small β_1 , make it difficult to draw any firm conclusions. The smaller values of B at large β_1 suggest that a reducing value of U_0 may be responsible, and this assumption would be in agreement with Tabakoff, who has shown that unlike stainless steel, the value of U_0 drops between $\beta_1 = 30$ and 60 deg. This reported variation, however, is not sufficiently large to explain the factor of 2 variation in B observed in these tests.

Values of k_1 and k_2

The magnitude of θ and B for both types of target material might be expected to shed some light on the values of k_1 and

k_2 , and U_0 and ω_0 . Clearly nothing exact can be attempted, but if we form the ratio $\tan\theta/B$, then k_2 is eliminated and we find, using $\tan\theta \approx 45$ deg, $B \approx 0.25$ m

$$U_0 \approx \omega_0 k_1 40 \times 10^{-6} \text{ m/s}$$

If it is assumed that the particle spins up during impact, it is reasonable to assume $U_0 \approx a\omega_0$. Thus, taking $a \approx 75 \mu\text{m}$, we obtain $k_1 = 1.4$. This value is between the values quoted by Maccoll and Rubinow and Keller for high and low Re , respectively. The value of k_1 , therefore, is not inconsistent with available data.

Taking B again as 0.25 m, we find from the expression for B that

$$U_0 \approx 1.5 \times 10^{-9} (k_2/a^2)$$

Taking $a = 75 \mu\text{m}$, we find

$$U_0 \approx 0.27 k_2 \text{ m/s}$$

Now the value of 8π for k_2 quoted earlier, based on very low Re flows, gives $U_0 \approx 6$ m/s, which is low by about an order of magnitude. All that can be done here is to suggest that $k_2 = 0(100)$. It can be deduced from the results of Sawatzki⁶ that the drag torque on a smooth sphere at $Re = 500$, in stationary fluid, is of the order of 5 times greater than that computed assuming $Re = 1$. It may be inferred that the values of B found from experiment are not physically improbable.

Table 2 Final results for aluminum target

β_1 , deg	Data points		Best fit curve constants			
	X , mm	Y , mm	β_2	θ	B , m	β_2/β_1
11	115	5.27	5.0	16.1	0.4	0.45
	185	7.73				
	300	3.27				
20	105	13.06	12.5	23.5	0.20	0.625
	195	9.16				
	340	0.29				
25	105	13.46	14.8	35.0	0.325	0.60
	195	16.76				
	340	0.97				
30	26	9.53	22.0	47.5	0.30	0.73
	50	8.85				
	75	12.95				
	105	17.51				
	185	23.03				
	187	18.69				
	232	14.44				
35	287	11.08	23.0	43.9	0.28	0.66
	325	1.56				
	347	3.27				
40	105	20.34	19.0	34.0	0.25	0.48
	195	24.30				
	340	10.41				
45	105	21.25	38.5	48.7	0.14	0.85
	195	32.18				
	340	9.94				
50	105	35.02	36.3	46.8	0.14	0.73
	195	33.78				
	340	27.09				

Table 1 Final results for stainless steel target

β_1 , deg	Data points		Best fit curve constants			
	X , mm	Y , mm	β_2	θ	B , m	β_2/β_1
12	40	4.69	12.7	35.3	0.25	1.06
	103	9.22				
	185	3.46				
20	40	7.36	16.1	34.4	0.252	0.81
	105	14.22				
	185	15.02				
	320	0.15				
30	40	9.40	19.1	39.9	0.275	0.64
	105	23.76				
	195	15.62				
	330	2.32				
40	40	13.52	22.7	43.0	0.238	0.57
	115	26.64				
	195	20.24				
50	40	14.20	21.3	40.0	0.273	0.43
	105	21.56				
	195	48.24				
	330	35.06				

Predictions of Theory in the Gas Turbine Environment

It is interesting to examine the behavior of smaller particles, $\sim 10 \mu\text{m}$, since these are more relevant to the gas turbine operating in the cleaned-up gas from a fluidized bed combustor.

From Eq. (5a), and writing $\omega_0 = U_0/a$, we see that A is proportional to aU_0 and inversely proportional to ν , assuming k, k_2 constant. In the gas turbine situation, using typical values for pressure temperature and velocity and taking $a \approx 10 \mu\text{m}$, we find that A is a factor of about 2 times less than in the experiments reported here. Thus, turning angles of the order of 20 deg may be involved in the gas turbine situation.

Examination of Eq. (5b) shows that the distance constant B is proportional to U_0 , ρ_{particle} and a^2 , and inversely proportional to ρ_{gas} and ν . Clearly, as in the calculation of A , typical gas turbine conditions have to be used in estimating B ; in addition, the particle density is required here. Taking typical values, it is found that B is about a factor of up to 30 less than that found in the present work, i.e., B is of the order of 20 mm or less in the gas turbine environment. These results suggest that accurate prediction of rebounding particles in a gas turbine require the effects of spin to be examined.

Conclusions

A simple method of determining particle trajectories after rebound has been described. This technique has enabled the average trajectory of rebounding particles to be studied in more detail than hitherto.

The results for particle impact with stainless steel and aluminum targets show that the rebounding particle has a

curved trajectory caused by a lift force produced by particle spin. The results presented for rebound angle are in general agreement with previously published work. Predictions from the theory suggest that spin effects on the trajectory of small particles in gas turbines can be significant.

Acknowledgments

This work was supported by the Science and Engineering Research Council and carried out in the Department of Mechanical Engineering, University of Nottingham.

References

- ¹Tabakoff, W., Kotwal, R., and Hamed, A., "Erosion Study of Different Materials Affected by Coal Ash Particles," *Wear*, Vol. 52, 1978, pp. 161-173.
- ²Tabakoff, W. and Balan, W., "Effects of Solid Particles Suspended in Fluid Flow Through an Axial Flow Compressor Stage," *5th International Symposium on Air Breathing Engines*, Bangalore, India, Feb. 1981, pp. 75.1-75.10.
- ³Tabakoff, W., Grant, E., and Ball, R., "An Experimental Investigation of Certain Aerodynamic Effects in Erosion," *Proceedings of the 8th AIAA Aerodynamic Testing Conference*, Md., 1974, pp. 1-14.
- ⁴Maccoll, J., "Aerodynamics of a Spinning Sphere," *Journal of the Royal Aeronautical Society*, Vol. 32, 1928, p. 777.
- ⁵Rubinow, S. I. and Keller, J. B., "Transverse Forces on a Spinning Sphere Moving in a Viscous Fluid," *Journal of Fluid Mechanics*, Vol. 11, 1961, pp. 447-459.
- ⁶Sawatzki, O., "Das Strömungsfeld um eine rotierende Kugel," *Acta Mechanica*, Vol. 9, 1970, p. 159.

From the AIAA Progress in Astronautics and Aeronautics Series . . .

TRANSONIC AERODYNAMICS—v. 81

Edited by David Nixon, Nielsen Engineering & Research, Inc.

Forty years ago in the early 1940s the advent of high-performance military aircraft that could reach transonic speeds in a dive led to a concentration of research effort, experimental and theoretical, in transonic flow. For a variety of reasons, fundamental progress was slow until the availability of large computers in the late 1960s initiated the present resurgence of interest in the topic. Since that time, prediction methods have developed rapidly and, together with the impetus given by the fuel shortage and the high cost of fuel to the evolution of energy-efficient aircraft, have led to major advances in the understanding of the physical nature of transonic flow. In spite of this growth in knowledge, no book has appeared that treats the advances of the past decade, even in the limited field of steady-state flows. A major feature of the present book is the balance in presentation between theory and numerical analyses on the one hand and the case studies of application to practical aerodynamic design problems in the aviation industry on the other.

696 pp., 6 × 9, illus., \$30.00 Mem., \$55.00 List

TO ORDER WRITE: Publications Order Dept., AIAA, 1633 Broadway, New York, N.Y. 10019